SHELXL-93, all hydrogen-atom positions were found in the Fourier map and freely refined, $C_{18}H_{26}Cl_4Cu_2N_{10}$, $M = 651.4\ g\,mol^{-1}$, orthorhombic, space group *Pbca* (no. 61), $a = 8.396(1)$, $b = 18.756(1)$, $c = 15.781(1)$ Å, $V = 2485.1(4)$ Å^3, $Z = 4$, $\rho_{calcd} = 1.741\ g\,cm^{-3}$, $\mu = 21.7\ cm^{-1}$, $T = 20\,^\circ C$, 30426 observed reflections, 1949 independent reflections used for refinement (1595 with $I > 4\sigma(I)$), 206 parameters refined, $R1 = 0.0255$, $\omega R2 = 0.0522$, GOF = 0.96, max./min. residual electron density 0.29/ − 0.25 e Å^{-3}.[12b]

[12] a) X-ray structure analysis of **3**: orange prisms from CH_2Cl_2/pentane, $Mo_{K\alpha}$ radiation ($\lambda = 0.71073$ Å), Enraf-Nonius MACH3 diffractometer, structure solution with Patterson methods (SHELXS-86), refinement with SHELXL-93, all hydrogen atoms were calculated in idealized positions, $C_9H_{13}Cl_2N_3Pd$, $M = 368.6\ g\,mol^{-1}$, monoclinic, space group $P2_1/n$ (no. 14), $a = 8.4828(6)$, $b = 9.4916(8)$, $c = 16.2852(15)$ Å, $\beta = 94.087(8)^\circ$, $V = 1307.9(2)$ Å^3, $Z = 4$, $\rho_{calcd} = 1.872\ g\,cm^{-3}$, $\mu = 18.1\ cm^{-1}$, $T = -110\,^\circ C$, 2735 observed reflections, 2644 independent reflections used for refinement (2086 with $I > 4\sigma(I)$), empirical absorption correction $T_{min} = 0.939\ T_{max} = 1.000$, 154 parameters refined, $R1 = 0.0534$, $\omega R2 = 0.0667$, $GOF = 1.05$, max./min. residual electron density 0.62/ − 0.69 e Å^{-3}. b) Crystallographic data (excluding structure factors) for the structures reported in this paper have been deposited with the Cambridge Crystallographic Data Centre as supplementary publication no. CCDC-101 257. Copies of the data can be obtained free of charge on application to CCDC, 12 Union Road, Cambridge CB2 1EZ, UK (fax: (+44) 1223-336-033; e-mail: deposit@ccdc.cam.ac.uk).

[13] The AM1 calculations were performed on a Silicon Graphics O2 Workstation with the MOPAC 6.0 package and the INSIGHT II Graphical User Interface (Biosym). a) M. J. S. Dewar, E. G. Zoebisch, E. F. Healy, J. J. P. Stewart, *J. Am. Chem. Soc.* **1985**, *107*, 3902 – 3909; b) M. J. S. Dewar, E. G. Zoebisch, *Theochem.* **1988**, *49*, 1 – 21; c) M. J. S. Dewar, C. Jie, E. G. Zoebisch, *Organometallics* **1988**, *7*, 513 – 521.

[14] A. L. Spek, *Acta Crystallogr. Sect. A* **1990**, *46*, C34 – C34.

[15] Y. G. Gololobov, L. F. Kasukhin, *Tetrahedron* **1992**, *48*, 1353 – 1406.

[16] J. R. Doyle, P. E. Slade, H. B. Jonassen, *Inorg. Synth.* **1960**, *6*, 216 – 219.

Covalent DNA – Streptavidin Conjugates as Building Blocks for Novel Biometallic Nanostructures**

Christof M. Niemeyer,* Wolfgang Bürger, and Jörg Peplies

The generation of nanoscale structural and functional devices by self-assembly of small molecular building blocks is an important goal of nanotechnology.[1] Owing to its unique recognition capabilities, physicochemical stability, and mechanical rigidity, DNA is a promising construction material[2–4] for the fabrication of nanostructured scaffolds[3] and for the precise spatial positioning of conducting polymers,[5] proteins,[6] and nanocrystalline gold clusters.[7–9] Recently, we reported the synthesis of covalent conjugates of single-stranded DNA and streptavidin (STV).[6] In these adducts, the protein's native binding capacity for four biotin molecules is supplemented by a highly specific binding site for complementary nucleic acids, and the conjugates can thus be utilized as biomolecular adapters for positioning biotinylated components along a nucleic acid backbone. Here we report on the self-assembly of DNA – STV adducts **3** to form supramolecular aggregates **5** and the utilization of the adapters for the fabrication of nanostructured biometallic aggregates **8** and **9** from biotin-derivatized metal colloids (Scheme 1).

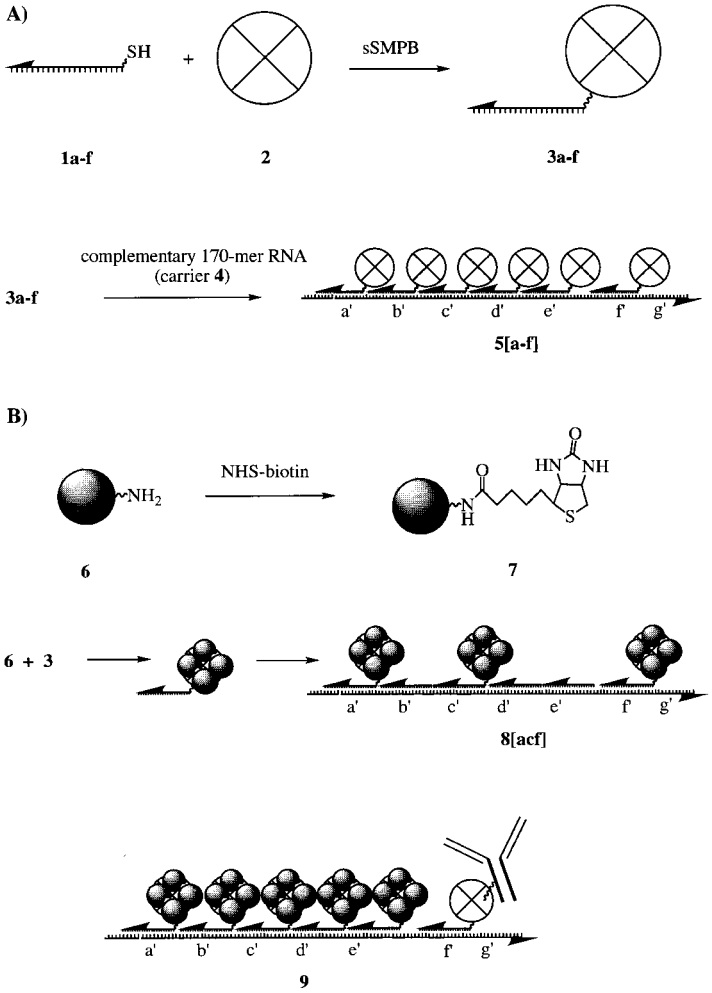

Scheme 1. Schematic representation of the DNA – protein hybrids. A) Generation of supramolecular aggregates from DNA – STV conjugates **3**, obtained by covalent coupling of 5′-thiol-modified oligonucleotides **1** and streptavidin **2**. The 3′-end of the oligonucleotide is indicated by an arrowhead, and the spacer chains between DNA and protein by wavy lines. The conjugates **3** with nucleotide sequences **a** – **f** self-assemble in the presence of RNA **4**, which contains complementary sequence sections, to form supramolecular aggregates **5**. B) Fabrication of biometallic aggregates by means of DNA – STV adapters **3**. Monoamino-modified 1.4-nm gold clusters **6** are converted into biotin derivatives, and the biotinylated clusters **7** are coupled with DNA – STV adducts **3.** The resulting hybrids are assembled in the presence of helper oligonucleotides **1** and RNA carrier **4** to form supramolecular aggregates **8**. (The letters in brackets indicate the protein components bound to the carrier.) Similarly, an antibody-containing aggregate **9** was constructed from gold-labeled **3a** – **e** and a conjugate from **3f** and biotinylated IgG, previously coupled in separate reactions.

[*] Dr. C. M. Niemeyer, Dipl.-Chem. W. Bürger, J. Peplies
Universität Bremen, FB2-UFT
Biotechnologie und Molekulare Genetik
Leobener Strasse, D-28359 Bremen (Germany)
Fax: (+49) 421-218-7578
E-mail: cmn@biotec.uni-bremen.de

[**] This work was supported by the Deutsche Forschungsgemeinschaft, the Fonds der Chemischen Industrie, and the Tönjes-Vagt Stiftung. We thank the staff of the Institut für Werkstoffphysik und Strukturforschung, Universität Bremen, for their help with the TEM imaging and Prof. D. Blohm for critical discussions and generous support.

  1433-7851/98/3716-2265 $ 17.50+.50/0

Six DNA – STV hybrid molecules **3** were synthesized from 5′-thiol-modified oligonucleotides with different base sequences **1a** – **f** and recombinant STV (**2**) by means of the heterobispecific cross-linker, sulfosuccinimidyl-4(*p*-maleimidophenyl)butyrate (sSMPB).[6] The nucleic acid sequences of the adapters **3a** – **f** were chosen from a region with about 170 base pairs of the antisense strand of bacteriophage M13mp18 DNA, and were recently studied with regard to their hybridization characteristics.[10] An RNA molecule **4** containing sequence sections complementary to **3a** – **f** in the order 5′-a′-b′-c′-d′-e′-f′-g′-3′ was prepared by in vitro transcription as a template for the supramolecular assembly of the adapters.

To investigate the organization of multiple protein components along the carrier molecule and to analyze the resulting aggregates **5**, an instrumental modification of the electrophoretic gel-shift assay,[11] widely applied for the study of biomolecular interactions, was designed. Labeling of the DNA – protein aggregates with a 5′-fluorescein-derivatized oligonucleotide probe (G18), which is complementary to binding site g′ of the RNA carrier, allows the DNA – protein aggregates to be analyzed with an automated DNA sequencer. Due to the high sensitivity and quantifiability of fluorescence detection, as well as a remarkably enhanced separation performance for compounds of high molecular weight compared to conventional electrophoresis, this method is highly suitable for the analysis of supramolecular DNA – protein aggregates and the investigation of the self-assembly processes.

In an initial series of experiments, the successive assembly of an aggregate of six DNA – STV adducts was investigated. A mixture of RNA carrier **4**, fluorescent probe G18, and an excess of hybrid **3a** (Figure 1 A, lane 1) showed bands of the free probe, the RNA – G18 heteroduplex, and a single species of higher molecular weight, which was assigned to the aggregate **4** · **3a** · G18. In spite of the excess of **3a**, no products with higher molecular weight are formed; this suggests that aggregation occurs exclusively by specific Watson – Crick base pairing. In contrast, the addition of further adducts complementary to the carrier strand, such as **3b** (Figure 1 A, lane 2), led to the formation of new species with lower electrophoretic mobility. Subsequently, supramolecular aggregates consisting of up to six protein components, that is, defined molecular assemblies with relative molecular weights of greater than 400 kDa were assembled (Figure 1 A, lanes 3 – 6). Quantification of the fluorescence bands indicated an increase in the aggregation yield with increasing number of bound conjugates **3**. This is an indication for cooperative effects during the self-assembly process, which are the result of increasing disruption of the secondary structures of the nucleic acid carrier and the associated increase in stability of the DNA – protein aggregates.[12] To further examine this phenomenon, several distinct aggregates were assembled and compared to control reactions in which free sequence stretches of the carrier backbone were saturated with "helper oligonucleotides" [12] (Figure 1 B). In the case of aggregates containing two protein components (e.g., **5[ad]** and **5[bd]**) the presence of helper oligonucleotides resulted not only in a doubling of the signal intensities, but also led to completion of the previously incomplete common aggregation of both protein components. These results

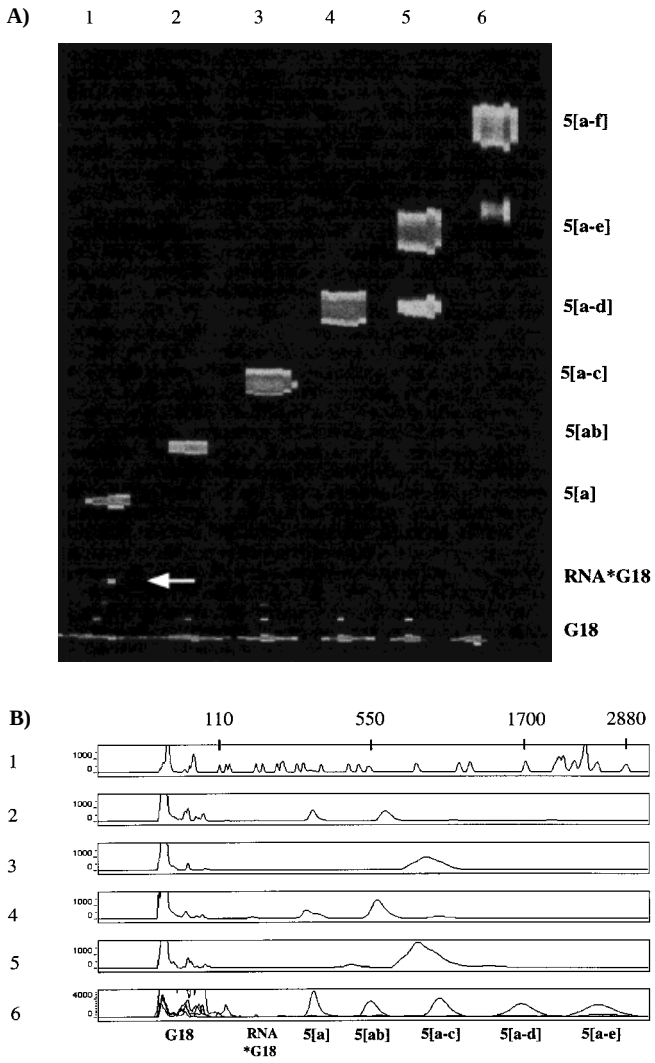

Figure 1. Investigaton of the supramolecular self-assembly of DNA – STV hybrids **3** by fluorescence gel-shift analysis. A) Lanes 1 – 6 correspond to successive construction of oligomeric aggregates **5**. The weak band of uncomplexed RNA **4** in lane 1 is indicated by an arrow. An increasing number of protein components bound to **4** leads to an increasing signal strength (gray scale representation of the originally blue fluorescence bands). Pentameric and hexameric DNA – protein aggregates (lanes 5 and 6) display enhanced dissociation, likely due to the absence of cations that stabilize the double helix during electrophoresis. B) Line plots of the gel-shift analysis of complexes **5[ad]** and **5[bd]** (lanes 2 and 4, respectively). The formation of ternary complexes is incomplete. Therefore, binary aggregates of similar electrophoretic mobility (**5[a]** and **5[d]**) are present in lane 2 in addition to the ternary aggregate **5[ad]**. The presence of helper oligonucleotides that are complementary to free sequence sections of the carrier leads to completion of aggregation and also reduces the electrophoretic mobility of **5[ad]** (lane 3) and **5[bd]** (lane 5). Lane 1: DNA molecular weight marker (GeneScan-2500 Rox, length in base pairs). Lane 6: overlay plot of five lanes for the successive assembly of a pentameric aggregate, analogous to the gel-shift analysis shown in A).

demonstrate that oligonucleotide-directed assembly of molecular devices can be significantly improved by minimizing secondary structure in the nucleic acid backbone.[13]

Stimulated by recent reports on oligonucleotide-directed organization of gold clusters,[7–9] we examined the applicability of biomolecular adapters **3** for the fabrication of nanostructured metal aggregates. For this purpose, preparative quantities of supramolecular aggregates **5** were prepared from

  1433-7851/98/3716-2266 $ 17.50+.50/0 *Angew. Chem. Int. Ed.* **1998**, *37*, No. 16

combinations of the individual DNA – STV components and separated from nonaggregated compounds by gel-filtration chromatography. Calibration of the filtration column gave approximate molecular weights of the aggregates **5[acf]** and **5[a – f]** of 240 and 440 kDa, respectively. Commercially available 1.4-nm gold clusters **6** with a single amino substituent were used as metal components. Following derivatization with *N*-hydroxysuccinimidylbiotin, the biotinylated metal colloids **7** were coupled to the DNA – STV adapters. The presence of gold particles within the protein hybrids was verified during chromatographic isolation by means of the characteristic absorption at 420 nm.

On analysis of the biometallic aggregates by transmission electron microscopy (TEM), multiple gold clusters bound to a single STV molecule could not be differentiated. Average particle sizes of 1.3 ± 0.2, 2.3 ± 0.3, 3.6 ± 0.3, and 4.5 ± 0.3 nm were observed, depending on the coupling stoichiometry between **3** and **7**. According to model calculations,[14] these dimensions are consistent with mono-, di-, tri-, and tetra-adducts of **7** with STV. Transmission electron micrographs of gold-labeled aggregates reveal stretched and sharply bent structures (Figure 2). Aggregates consisting of three protein components, **8[acf]**, have particle sizes of 4.5 nm and two different interparticle distances of approximately 5 ± 2 and 10 ± 3 nm (Figure 2A). These results are in agreement with the schematic aggregate structure (Scheme 1), since both nucleic acid spacer regions are flexible due to the presence of several gaps in the backbone of the double helix.

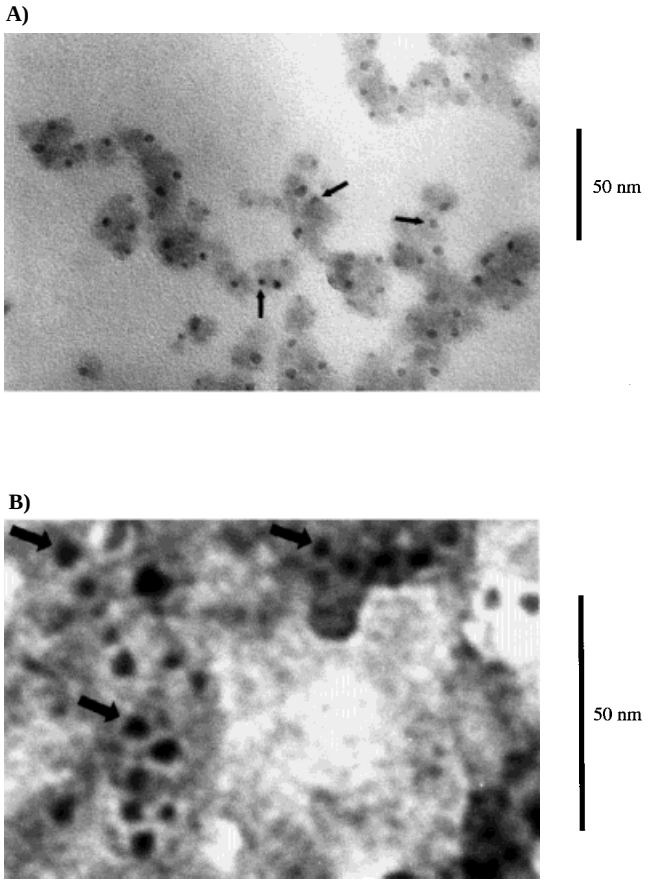

Figure 2. TEM images of supramolecular aggregates labeled with gold clusters. A) DNA – protein aggregate containing three DNA – STV adapters **8[acf]**. The central particles of typical aggregates are indicated by arrows. B) Aggregate **9** containing five gold-labeled adapters **3a – e**, anti-mouse IgG-coupled **3f**, and RNA. Since optical differentiation of the four STV-bound clusters was not achieved, the individual gold-labeled adapters are visible as spherical structures of high contrast. The shady areas in the background result from immobilized protein matrices (poly-D,L-lysine in A) and mouse IgG in B).

Subsequently a functional protein component was incorporated into the biometallic aggregates. To generate the IgG-containing construct **9** (IgG = immunoglobulin), DNA – STV hybrid **3f** was coupled with a biotinylated antibody against IgG from mice, and hybrids **3a – e** were coupled with biotinylated gold clusters. Following organization of the components along RNA carrier **4** and subsequent chromatographic purification, the functionality of the product aggregate was tested by coating TEM grids with mouse IgG and briefly bringing them into contact with a solution of **9**. In control experiments with grid-immobilized rabbit IgG, no metal colloids were observed, but TEM images of antigen-coated surfaces showed clear accumulations of clusters in which isolated chainlike structures were evident (Figure 3B). The metal aggregates have average particle sizes and interparticle distances of 4.6 ± 0.3 and 2.7 ± 0.4 nm, respectively. This leads to an estimated length of the nucleic acid domain within single DNA – STV components of about 7.3 nm, which is consistent with the theoretical value of 7.1 nm of a double helix with 21 base pairs. The length of the three chainlike structures is 33 ± 2 nm, which correlates with the theoretical value of about 37 nm for a double helix with 108 base pairs when the flexibility of the 1.2-nm spacers between oligonucleotide and STV is taken into account.

These experiments demonstrate the applicability of covalent conjugates of oligonucleotides and streptavidin as versatile and convenient adapters for the fabrication of novel nanostructured molecular assemblies. Further fundamental studies of structure, stability, formation, and modification of supramolecular aggregates based on nucleic acids will show whether biotechnological applications such as sensor and switching devices, synthetic multienzyme complexes, and interface structures between electronic and biological systems can be realized.

Experimental Section

Covalent DNA – STV Adducts were synthesized from 5′-thiolated oligonucleotides (NAPS, Göttingen) and recombinant STV (Boehringer Mannheim) by means of the heterobispecific cross-linker sSMPB (Pierce) in about 10 – 15% yield.[6] The nucleotide sequences of **1a – f** are as follows: 5′-thiol-TCC TGT GTG AAA TTG TTA TCC GCT-3′ (**1a**); 5′-thiol-GTA ATC ATG GTC ATA GCT GTT-3′ (**1b**); 5′-thiol-CCG GGT ACC GAG CTC GAA TTC-3′ (**1c**); 5′-thiol-CAG GTC GAC TCT AGA GGA TCC-3′ (**1d**); 5′-thiol-AGT GCC AAG CTT GCA TGC CTG-3′ (**1e**); 5′-thiol-GTT TTC CCA GTC ACG ACG TTG TAA-3′ (**1f**). For the preparation of RNA carrier **4**, a double-stranded DNA fragment with 189 base pairs was synthesized from M13mp18 DNA by polymerase chain reaction (PCR) with primers M13T7 (5′-GTA ATC ATG GTC ATA GCT GTT-GTA ATC ATG GTC ATA GCT GTT-3′) and M13G3 (5′-GTA ATC-ATG GTC ATA GCT-3′). Primer M13T7 contains the promoter region of T7-RNA polymerase (underlined). In vitro transcription of the purified PCR product yields approximately 10 molar equivalents of the corresponding 170-mer RNA. The latter was characterized by conventional

  1433-7851/98/3716-2267 $ 17.50+.50/0

electrophoresis (10% acrylamide gel containing 7 M urea) in the presence of a DNA molecular weight standard (GIBCO).

Fluorescence gel-shift analysis was carried out with an ABIPrism 377 DNA sequencing instrument (Perkin Elmer). The nucleotide sequence of the 5′-fluorescein-derivatized G18 oligonucleotide probe (NAPS) is 5′-fluorescein-GTA ATG GTC ATA GCT GTT-3′. In a typical experiment, 3 pmol of the hybrid component (3 μM stock solution in tris(hydroxymethyl)aminomethane (tris) buffer, pH 7.3, 150 mM NaCl) was mixed with 0.5 pmol of RNA **4** and 0.5 pmol of G18 probe and the mixture incubated for 30 min at 37 °C. If no temperature-sensitive components are present, the aggregation may also be carried out for 2 min at 50 °C. A volume of 1 μL of the mixture was applied to a nondenaturing 4% acrylamide gel, and electrophoresis was carried out at 750 V, 50 mA for 3.5 h at 20 °C. The fluorescence bands were analyzed with ABI Prism GeneScan 2.0.2 software (Perkin Elmer).

Amino-modified 1.4-nm gold clusters (20 nmol; Monoamino-Nanogold, Nanoprobes) in 100 μL of phosphate buffer were treated with 10 equiv of NHS-biotin (Pierce) for 60 min at room temperature and subsequently purified by chromatography on a Superdex Peptide FPLC column (Pharmacia). Coupling with **3** was performed by mixing typically 100 pmol of the DNA–STV hybrids with 2–8 molar equivalents of **7** followed by incubation for 60 min. The assembly was carried out by the addition of 100 pmol of RNA **4** and incubating the mixture for 60 min. In some cases, unlabeled aggregates **5** were prepared and purified by chromatography (Superdex-200, Pharmacia) and subsequently treated with **7**. The purified biometallic aggregates were concentrated by ultrafiltration (Centricon, Millipore) and quantified photometrically. To prepare aggregate **9**, **3a–e** were coupled with **7** and **3f** with biotinylated goat anti-mouse IgG (Dianova) in separate reactions prior to the addition of RNA. For TEM analysis, 400-mesh copper grids with a thin carbon coating (Plano) were coated with proteins (mouse or rabbit IgG or poly-D,L lysine, Boehringer-Mannheim, 1 mg mL^{-1} in phosphate-buffered NaCl solution). For immobilization, a 5-μL drop of the gold-labeled aggregates (1–10 nM) was deposited on the grids for 2 min. TEM analysis was carried out with a Philipps EM 420 instrument operating at 120 kV.

Received: December 29, 1997
Revised version: April 9, 1988 [Z11301IE]
German version: *Angew. Chem.* **1998**, *110*, 2391–2395

Keywords: DNA hybridization · nanostructures · supramolecular chemistry

[1] a) R. P. Feynman in *Miniaturization* (Ed.: H. D. Gilbert), Reinhold, New York, **1961**, p. 282; b) K. E. Drexler, *Proc. Natl. Acad. Sci. USA* **1981**, 78, 5275; c) J.-M. Lehn, *Supramolecular Chemistry*, VCH, Weinheim, Germany **1995**, p. 193; d) D. Philp, J. F. Stoddart, *Angew. Chem.* **1996**, 108, 1242; *Angew. Chem. Int. Ed. Engl.* **1996**, *35*, 1154.
[2] N. C. Seeman, *J. Theor. Biol.* **1982**, *99*, 237.
[3] N. C. Seeman, *Acc. Chem. Res.* **1997**, *30*, 357.
[4] C. M. Niemeyer, *Angew. Chemie* **1997**, *109*, 603; *Angew. Chem. Int. Ed. Engl.* **1997**, *36*, 585.
[5] B. H. Robinson, N. C. Seeman, *Protein Eng.* **1987**, 1, 295.
[6] C. M. Niemeyer, T. Sano, C. L. Smith, C. R. Cantor, *Nucl. Acids Res.* **1994**, *22*, 5530.
[7] C. A. Mirkin, R. L. Letsinger, R. C. Mucic, J. J. Storhoff, *Nature* **1996**, *382*, 607.
[8] A. P. Alivisatos, K. P. Johnsson, X. Peng, T. E. Wilson, C. J. Loweth, M. P. Bruchez Jr., P. G. Schultz, *Nature* **1996**, *382*, 609.
[9] R. Elghanian, J. J. Storhoff, R. C. Mucic, R. L. Letsinger, C. A. Mirkin, *Science* **1997**, *277*, 1078.
[10] A comparative study of the hybridization kinetics of **1a–f** and **3a–f** revealed dramatic differences in affinity of sequences **a–f**: The hybridization efficiency at room temperature decreases in the order **a** > **b**, **f** > **c**, **d** > **e** and correlates with the structural properties of the oligonucleotides. The coupling with STV results in minor changes of the sequence-specific binding properties: The rates of association and dissociation of **3a–f** are up to five times slower than those of **1a–f**. C. M. Niemeyer, W. Bürger, R. J. M. Hoedemakers, *Bioconjugate Chem.* **1998**, *9*, 168.
[11] *Current Protocols in Molecular Biology, Vol. 2*, Wiley, New York, **1996**.
[12] This effect was previously observed, for example, for the binding of 12-mer oligonucleotides to an RNA molecule: G. Godard, J.-C. Francois, I. Duroux, U. Asseline, M. Chassignol, N. Thuong, C. Helene, T. Saison-Behmoaras, *Nucleic Acids Res.* **1994**, *22*, 4789.
[13] Although the denaturation temperature of STV is higher than 75 °C (M. González, L. Bagatolli, I. Echabe, J. Arrondo, C. Argaraña, C. R. Cantor, G. Fidelio, *J. Biol. Chem.* **1997**, 11288), due to the thermal instability of many biomolecules and the gold clusters **6**, the oligonucleotide-directed assembly of proteins requires moderate temperatures. The RNA **4** forms secondary structures at these temperatures with similar stability ($\Delta G \approx -44.6$ kcal mol^{-1}) to the oligonucleotide double helices ($\Delta G = -34.2$ to -44.7 kcal mol^{-1}[10]). Thus, thermodynamic stability of binary aggregates **5** is, depending on the sequences, influenced to a varying extent by the presence of helper oligonucleotides. Experiments in which the aggregation temperature and time were varied suggest that the system reaches thermodynamic equilibrium under the conditions described. Therefore, the influence of helper oligonucleotides depends on the base sequence and the number of DNA–STV hybrids. While the formation of binary aggregates is increased by a factor of up to 20 (e.g., for **5[d], 5[e]**), depending on the sequence, a comparison of ternary aggregates reveals an increase in signal intensity by a factor of up to three, depending on the building blocks applied. The rates of increase are consistent with the calculated secondary structure of **4**, and this indicates that the sequence section d′-e′-f′, in particular, is engaged in a stable double-helical domain. Aggregates consisting of four or more protein components are scarcely influenced by helper oligonucleotides.
[14] The dimensions of the protein are approximately 4 × 4.2 × 5.6 nm, and the four biotin-binding sites inside the molecule form a distorted tetrahedron with edge lengths of about 2.3 nm on average: P. C. Weber, D. H. Ohlendorf, J. J. Wendoloski, F. R. Salemme, *Science* **1989**, *243*, 85. After labeling of avidin with similar 1-nm gold clusters, a distance between the biotin binding sites of about 2 nm was determined: D. E. Safer, J. Hainfeld, J. S. Wall, J. E. Reardon, *Science* **1982**, *218*, 290.

Synthesis of an ansa-Zirconocene via a Novel S_4-Symmetric Spirobis(silastannaindacene) Compound**

Mario Hüttenhofer, Frank Schaper, and Hans H. Brintzinger*

The utilization of chiral ansa-zirconocenes as catalysts for numerous reactions[1, 2] demands a diastereoselective synthetic access to these complexes.[3] One approach to this goal involves the diastereoselective reaction of $ZrCl_4$ with a silyl-bridged bis(cyclopentadienylstannyl) ligand unit[4, 5] or a substituted 8-sila-4-stannatetrahydroindacene, a cyclic stan-

[*] Prof. H. H. Brintzinger, M. Hüttenhofer, F. Schaper
Fakultät für Chemie der Universität
Fach M 737, 78457 Konstanz (Germany)
Fax: (+49) 7531-883-137
E-mail: hans.brintzinger@uni-konstanz.de

[**] ansa-Metallocene Derivatives, part 42. This work was supported by BASF AG, BMBF, and the Fonds der Chemischen Industrie. We thank Dr. Armin Geyer and Monika Cavegn for NMR spectra. Part 42: S. Martin, H. H. Brintzinger, *Inorg. Chim. Acta*, in press

Supporting information for this article is available on the WWW under http://www.wiley-vch.de/home/angewandte/ or from the author.

  1433-7851/98/3716-2268 $ 17.50+.50/0